Available online at www.sciencedirect.com
ScienceDirect
Thin Solid Films 517 (2008) 1077–1080
www.elsevier.com/locate/tsf

Characterization of ZnO and ZnO:Al thin films deposited by the sol–gel dip-coating technique

R.E. Marotti [a,*], C.D. Bojorge [b], E. Broitman [c], H.R. Cánepa [d], J.A. Badán [a], E.A. Dalchiele [a], A.J. Gellman [c]

[a] Instituto de Física, Facultad de Ingeniería, Universidad de la República, J. H. Reissig 565, CC 30, CP 11000, Montevideo, Uruguay
[b] REPSOL-YPF, CITEFA, CINSO, Juan B. de La Salle 4397 — CP 1603 Villa Martelli, Buenos Aires, Argentina
[c] Department of Chemical Engineering, Carnegie Mellon University, Pittsburgh PA 15213, USA
[d] CINSO, CONICET-CITEFA, Juan B. de La Salle 4397, CP 1603 Villa Martelli, Buenos Aires, Argentina

Available online 15 June 2008

Abstract

Nanocrystalline zinc oxide films have been obtained by the sol–gel process. The films were deposited from precursor solutions by dip-coating on quartz substrates, and subsequently transformed into nanocrystalline pure or aluminium-doped ZnO films after a thermal treatment. The film microstructure and composition characterization was studied by X-ray diffraction (XRD) and X-ray photoelectron spectroscopy (XPS). The optical properties were studied by transmittance spectroscopy. The water adsorption energy was measured by temperature programmed desorption (TPD) in the range 90–700 K. The optical transmittance in the UV region gives bandgap energy values of 3.27 eV for undoped samples, and higher than 3.30 eV for the Al-doped ones. The increase in bandgap energy in Al-doped samples may be explained by band-filling effects. The band edge absorption coefficient increases monotonically for the Al-doped samples but has a shoulder for the undoped ones, which may be assigned to room-temperature excitonic absorption.

Keywords: Zinc oxide; Optical properties; Doping; Thin films; Sol–gel; Temperature programmed desorption

1. Introduction

During the last years there has been a renewed interest in ZnO-based electronic and optoelectronic devices. With a wide bandgap of 3.4 eV and a large exciton binding energy of 60 meV at room temperature, ZnO could be important in the development of blue and ultra violet optical devices [1,2]. Furthermore, the use of thin film technology has opened the field to the fabrication of high quality material for applications such as UV light emitters, detectors, gas sensing elements, nanoheterojunctions, and even catalysts. With reduction in size, novel electrical, mechanical, chemical, and optical properties could be introduced in nanostructured ZnO films [3].

It is well known that the water in the environment reacts with the surface of ZnO single crystals [4]. The interaction of water with Zn films has also been used for the preparation of ZnO films by wet oxidation [5,6]. However, to our knowledge, there is no information regarding the interaction of water with nanocrystalline ZnO films.

In this paper we study the structure, composition, and optical properties of nanocrystalline ZnO and ZnO:Al films deposited by a sol–gel process. The room-temperature exciton absorption dependence with Al doping is observed. Also, the interaction of water with ZnO films is measured by temperature programmed desorption experiments.

2. Experimental procedure

2.1. Sample preparation

Nanocrystalline zinc oxide films have been obtained by the sol–gel process. ZnO precursor solution was prepared using zinc acetate dihydrate in ethyl alcohol as a starting material.

* Corresponding author.
E-mail address: khamul@fing.edu.uy (R.E. Marotti).

0040-6090/$ - see front matter © 2008 Elsevier B.V. All rights reserved.
doi:10.1016/j.tsf.2008.06.028

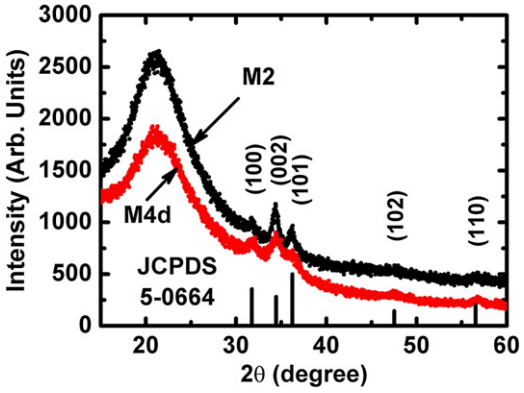

Fig. 1. XRD for two selected samples: M2 (undoped) and Md4 (Al doped). The lines at the bottom show the JCPDS for ZnO [10].

Acetic acid as a product of the hydrolysis reaction and deionized water were also added. The solution was aged at 65 °C during 2 h.

In the case of the doped films, solution was prepared by adding aluminium nitrate nanohydrate, before the ageing, in a molar ratio Al/Zn = 5%. Diethanolamine and acetylacetone were incorporated in order to control the ZnO colloids size and stabilize the sol. The precursor solutions were deposited by dip-coating technique on amorphous SiO_2 substrates and dried at room temperature, repeating the procedure for each layer. Amorphous zinc oxide and other species are transformed into nanocrystalline pure or Al-doped ZnO after thermal treatments.

2.2. Sample characterization

Sample microstructure was analyzed by XRD using a PW 3710 Philips diffractometer with Cu-K_α radiation, operating with glancing angle geometry. The angle of incidence used was 1° (the critical angle varies in the range 0.25–0.30°).

Both XPS and TPD experiments were conducted in an ultrahigh vacuum (UHV) stainless steel chamber with a base pressure of $\sim 2\times10^{-10}$ Torr. The chamber was equipped to perform Ar^+ ion sputtering, XPS and TPD [7]. ZnO samples (approximately 12×12 mm^2 in size) were mounted onto a Ni foil holder that was spot-welded between two tantalum heating wires attached to the liquid nitrogen cooled sample holder at the bottom of a UHV manipulator. The sample temperature was measured using a chromel–alumel thermocouple that was attached to the back of the Ni foil and controlled via computer feedback to a DC heating supply.

Carbon contamination was removed from the surface by Ar^+ ion sputtering. Typically, the surface was sputtered with 1.0 keV argon ions during 3 min at 300 K. Surface cleanliness was verified by XPS.

TPD experiments in the range 100–500 K were done by cooling the ZnO sample with liquid nitrogen to less than 100 K. The surface was then exposed to water admitted into the chamber through a leak valve. Desorption measurements were performed by heating the sample at a constant rate of 0.5 K/s while the mass spectrometer monitored the species desorbing from the surface. The mass spectrometer is housed in a metal tube which terminates in a circular aperture approximately 8 mm in diameter. Desorption experiments were conducted with the sample approximately 3–5 mm from the end of this aperture, and any desorption from the opposite side of the sample is undetectable. The result of the TPD experiment is a plot of desorption rate as a function of sample temperature. Using the peak desorption temperatures, T_p, and the heating rate, the desorption energies, E_{des}, can be estimated using the relationship developed by Redhead [8].

The optical properties were studied at room temperature by transmittance spectroscopy using the same system as in a previous work [9]. It uses a Xe lamp (ORIEL 6262) light source, whose output is chopped with an SRS SR540 chopper and filtered with an ORIEL 77250 monochromator. A UDT 11-09-001-1 linearized photodiode detects the light going across the sample and two lock-in amplifiers (an SRS SR530 and an EG&G 5209) recover the signal. A bare substrate similar to the one where each sample is grown is used as a reference for calculating the ZnO thin films transmittance.

3. Results and discussion

Two distinct features are present in XRD spectra showed in Fig. 1: a broad low angle (10°–30°) structure, originated in the amorphous substrate, plus small and wide diffraction peaks. These peaks appear very close to the characteristic wurtzite structure for the ZnO [9].

3.1. XPS analysis

Fig. 2 shows the representative XPS full spectra of clean (a) ZnO and (b) ZnO:Al thin films The Al2p, O1s, Zn2p3/2 and Zn2p1/2 peaks can be easily observed. The binding energies were calibrated by taking Zn2p3/2 peak (1021.9 eV) as reference. The atomic concentration of Al, O and Zn were computed from the measured peak area together with the following sensitivity factors: Al: 0.234; O: 0.711; Zn: 3.726.

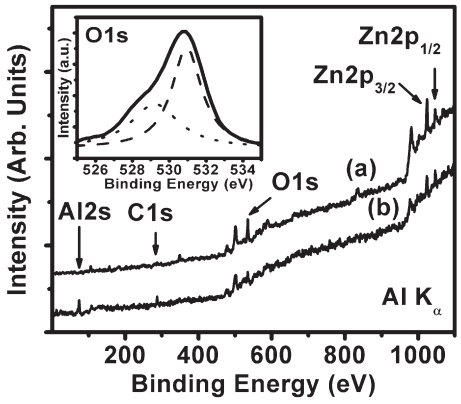

Fig. 2. XPS spectra of clean (a) ZnO and (b) ZnO:Al thin films. The Al2p, O1s, Zn2p3/2 and Zn2p1/2 can be easily observed. Other observed peaks correspond to Auger transitions. The inset shows O1s signal of ZnO thin films. The curve can be resolved into two peaks by a Lorentzian distribution fitting. (Anode: Al K_α 1486.6 eV).

The ratio of Zn and O of the ZnO film resulted 0.53 while the ratio of Al to Zn resulted 0.04.

The O1s signal shown in the inset of Fig. 2 has been resolved into two peaks by a Lorentzian distribution fitting. The peak with low binding energy (529.2 eV) corresponds to O^{2-} on normal wurtzite structure of ZnO single crystal [11]. Another peak centered at 532.0 eV is attributed to O^{2-} in the oxygen deficient regions within the matrix of ZnO [12].

3.2. TPD analysis

Fig. 3 displays TPD data obtained from a clean ZnO surface exposed to different doses of water measured in units of Langmuir ($L=1\times10^{-6}$ mbar s). It is observed that, at low coverage, water desorption does not show perfect zero-order desorption. As the coverage is increased the maximum desorption temperature shifts to higher values, whilst the desorption traces share the same low temperature leading edge, indicative of zero-order behavior: the adsorbate–adsorbate interactions are stronger than adsorbate–surface interactions. Zwicker et al. [4] studied the TPD of water on single-crystal ZnO. They found the presence of multiple peaks at different temperatures. The peaks at low temperature (150–170 K) were interpreted as the formation of two and three-dimensional ice, while the peaks at higher temperature (190–340 K) were assigned to site-specific interactions of adsorbed water with zinc sites and with oxygen sites on ZnO (0001). There are no published results of water adsorption on ZnO poly or nanocrystalline materials. Our results show the presence of one peak at the low temperature range. From our data, the adsorption energy of water on ZnO is calculated as $E_{des}=12.2\pm0.3$ kcal/mol, slightly higher than the water's combined heats of vaporization and fusion: $\Delta H_v+\Delta H_f=9.72$ kcal/mol+1.44 kcal/mol.

3.3. Optical properties

Fig. 4 shows the transmittance of selected ZnO thin films. In the visible region (400 to 600 nm) the spectra are almost flat showing no particular structure. The transmittance is close to 90% at 600 nm; i.e. the samples are quite transparent at the visible region. Close to 380 nm a shoulder indicates the onset of an absorption band edge. Into the UV region the transmittance diminishes but still remains higher than 50% in all cases. The ZnO thin film transmittance reported in the literature is expected to vanish at the UV [13,14]. However, as in the present case, when the films have a nanometric thickness (between 20 to 30 nm) there is not enough optical path for vanishing transmittance [9,15]. Moreover, it was already shown that for the undoped samples a direct correlation could appear among the thickness, number of layers, and UV transmittance value, although this is not the general case [9].

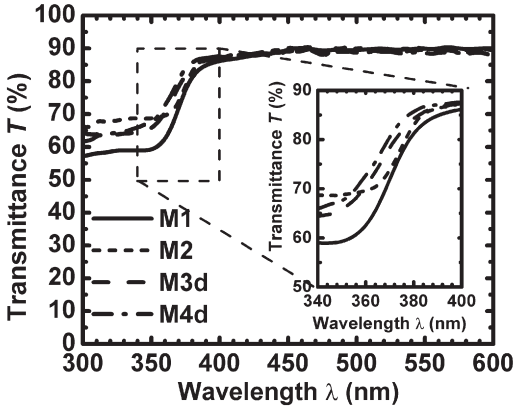

Fig. 4. Transmittance spectra of selected samples: M1 and M2 undoped, thermal treatment at 450 °C, with 6 and 4 layers respectively. M3d and M4d 5% Al doped with thermal treatments at 450 °C and 350 °C, respectively, with 6 layers both. Inset shows the region close to onset of absorption in detail.

The inset of Fig. 4 shows a zoom of the absorption edge region. For the doped samples the edge is smoother than the one for undoped samples. Fig. 5 shows the absorbance spectra ($\alpha d=-\ln T$ being α the absorption coefficient, d film thickness and T transmittance) [16]. The difference between doped and undoped samples is clearly seen in this figure: while absorption in doped samples increases smoothly from the visible into the UV, for undoped samples the absorption spectra has a step-like

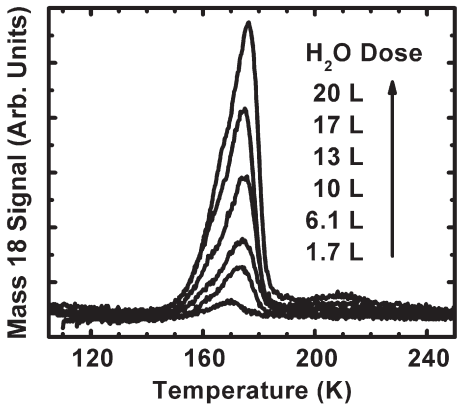

Fig. 3. TPD spectra recorded following increased exposures of water on a clean ZnO sample initially at 100 K.

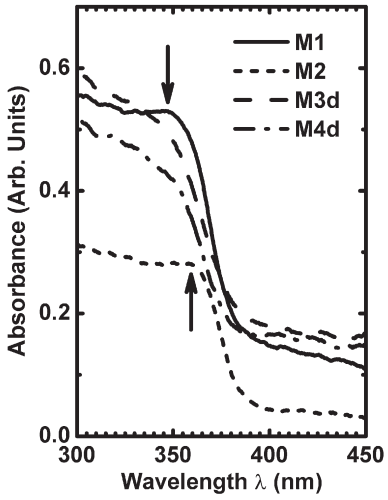

Fig. 5. Absorbance against wavelength close to absorption edge. The spectrum corresponding to sample M2 is shifted downward for clarity.

behavior. In this last case a shoulder is detected (indicated by vertical arrows for samples M1 and M2 in Fig. 5), that is not present in any doped samples. This structure may be attributed to room-temperature exciton absorption [16], which can be observed in ZnO because the exciton binding energy (E_b) is higher than the room-temperature thermal energy (k_BT): E_b= 60 meV > k_BT=26 meV [2]. For the doped samples, this shoulder is not seen. Moreover, the same difference in spectral shape due to doping effects is expected by comparison of previous works [16,17]. The intensity of this structure was used as indication of solid undoped ZnO [16], while for Al-doped ZnO the structure is smoother and tends to disappear with the increase of Al content [17]. Hence, the absence of this shoulder is an indication of the correct incorporation of the Al specie as a dopant into the ZnO samples.

To further study the absorption edge, the bandgap energies were calculated by the usual extrapolation of a linear fitting in $(\alpha \times h\nu)^2$ vs. photon energy $h\nu$ plots, after subtracting a proper background for any residual below bandgap energy absorption [9]. The obtained values may be influenced by shifts due to nanocrystal size effects [9]. The mean room-temperature "bulk" bandgap energy value obtained for undoped samples results 3.27±0.01 eV. This is close to the usually reported values for undoped ZnO [18]. For samples grown with 5% Al/Zn content the corresponding value is 3.325 eV±0.025 eV, although if only samples with thermal treatment at 450 °C are considered it is 3.315 eV±0.015 eV. Therefore, there is a shift of the absorption edge due to doping effect on the order of 0.5 eV.

The absence of the exciton peak and corresponding UV shift of the absorption spectra may be attributed to two different reasons: quantum size shift due to nanocrystalline size [3] and band-filling effects because of Al incorporation into the films [19]. The former one was already studied in a previous paper [9], but the shift due to Al content is an evidence that Burstein–Moss effect is being observed in the present samples and should be responsible for the disappearance of the exciton absorption in Al-doped samples.

4. Conclusions

Undoped and Al-doped ZnO thin films were obtained by sol–gel dip-coating technique, with nanometric thickness and typical wurtzite structure. XPS analysis shows that the material is defective in oxygen. TPD analysis shows that the nanocrystalline ZnO is chemically less active than single-crystal ZnO. The interaction with adsorbed water is very weak, with an adsorption energy E_{des} of 12.2 kcal/mol.

The samples show typical optical spectra of ZnO thin films in the order of tens of nanometer thick. For undoped samples the absorptance spectra shows a step-like behavior with a shoulder that can be assigned to room-temperature exciton absorption. This shoulder is not present for aluminum doped samples. The bandgap energy for undoped samples has a mean value of 3.27± 0.01 eV, while the mean bandgap energy for 5% Al/Zn (in solution) and thermal treatment at 450 °C is 3.315±0.015 eV. Therefore, both XPS and optical properties show that Al is being incorporated as a dopant in ZnO thin films.

Acknowledgments

C. D. B. and H. R. C. thank the Fundación YPF and CONICET, Argentina, for providing financial support during the work. J. A. B., E. A. D. and R. E. M. acknowledge the support received from PEDECIBA — Física, and the CSIC (Comisión Sectorial de Investigación Científica) of the Universidad de la República, in Montevideo, Uruguay. The authors also acknowledge Prosul program from CNPq (Brazil).

References

[1] Y.F. Chen, H.J. Ko, S.K. Hong, T. Sekiuchi, T. Yao, Y. Segawa, J. Vac. Sci. Technol., B 18 (2000) 1514.
[2] Ü. Özgür, Y.I. Alivov, C. Liu, A. Teke, M.A. Reshchikov, S. Doğan, V. Avrutin, S.J. Cho, H. Morkoç, J. Appl. Phys. 98 (2003) 041301.
[3] E.M. Wong, P.C. Searson, Appl. Phys. Lett. 74 (1999) 2939.
[4] G. Zwicker, K. Jacobi, J. Cunningham, Int. J. Mass Spectrom. Ion Process. 60 (1984) 213.
[5] Z.W. Li, W. Gao, Thin Solid Films 515 (2007) 3323.
[6] Zhengping Fu, Zhen Wang, Beifang Yang, Yingling Yang, Hongwei Yan, Linsheng Xia, Mater. Lett. 61 (2007) 4832.
[7] Y. Yun, E. Broitman, A.J. Gellman, Langmuir 23 (2007) 1953.
[8] P.A. Redhead, Vacuum 12 (1962) 203.
[9] C.D. Bojorge, H.R. Cánepa, U.E. Gilabert, D. Silva, E.A. Dalchiele, R.E. Marotti, J. Mater. Sci., Mater. Electron. 18 (2007) 1119.
[10] JCPDS, 5-0664, ZnO, 1992.
[11] B.J. Coppa, R.F. Davis, R.J. Nemanich, Appl. Phys. Lett. 82 (3) (2003) 400.
[12] M. Chen, X. Wang, Y.H. Yu, Z.L. Pei, X.D. Bei, C. Sun, R.F. Huang, L.S. Wen, Appl. Surf. Sci. 158 (2000) 134.
[13] D. Bao, H. Gu, A. Kuang, Thin Solid Films 312 (1998) 37.
[14] E.A. Dalchiele, P. Giorgi, R.E. Marotti, F. Martín, J.R. Ramos-Barrado, R. Ayouci, D. Leinen, Sol. Energy Mater. Sol. Cells 70 (2001) 245.
[15] K. Keis, A. Roos, Opt. Mater. 20 (2002) 35.
[16] L. Znaidi, G.J.A.A. Soler Illia, S. Benyahia, C. Sanchez, A.V. Kanaev, Thin Solid Films 428 (2003) 257.
[17] G.G. Valle, P. Hammer, S.H. Pulcinelli, C.V. Santilli, J. Eur. Ceram. Soc. 24 (2004) 1009.
[18] R. Bhargava, Wide bandgap II–VI semiconductors, EMIS Datareviews Series No 17 (INSPEC, London, 1997), p. 27 and p. 179.
[19] B.E. Sernelius, K.F. Berggren, Z.C. Jin, I. Hamberg, C.G. Granqvist, Phys. Rev. B 37 (1988) 10244.